



Cite this: *Green Chem.*, 2023, **25**, 3995

# Sustainable keratin recovery process using a bio-based ionic liquid aqueous solution and its techno-economic assessment†

Cariny Polesca, <sup>a,b</sup> Amir Al Ghatta, <sup>b</sup> Helena Passos, <sup>a</sup> João A. P. Coutinho, <sup>a</sup> Jason P. Hallett <sup>\*b</sup> and Mara G. Freire <sup>\*a</sup>

Keratin is a biopolymer with high potential for biomaterial production, being principally investigated in hydrogel and film forms for use in tissue-engineering applications. Aiming to find sustainable solvents and develop an efficient keratin recovery process, this work used an aqueous solution of bio-based ionic liquid (IL) for the dissolution of chicken feathers. Complete dissolution of chicken feathers in an aqueous solution of cholinium acetate ( $[\text{N}_{111}(\text{2OH})][\text{C}_1\text{CO}_2]$ ) was conducted at a solid : liquid weight ratio of 1 : 20 w/w, 100 °C for 4 h. An experimental design was carried out to optimize the keratin recovery conditions, investigating coagulant solvent, solution : coagulant weight ratio, and time. Under the optimal conditions (20.25 wt% of ethanol in water, 5 h, and solution : coagulant ratio of 1 : 1.45 w/w), 93 wt% of keratin was recovered. The IL was shown to be reusable in four successive cycles, with a yield of around 95 wt% and no significant losses in the efficiency of keratin recovery. These results demonstrate that an aqueous solution of  $[\text{N}_{111}(\text{2OH})][\text{C}_1\text{CO}_2]$  can lead to effective keratin recovery, serving as the basis for the development of a more effective and environmentally friendly process to recover biopolymers from waste. Due to the relevance of the developed process, techno-economic assessment through a comprehensive sensitivity analysis was carried out, evaluating a virtual operating biorefinery and showing a pathway that can enable the commercialization of produced keratin by the developed process. According to the process simulation, the minimum selling price for keratin is 22 \$ per kg, with a small positive  $\text{CO}_2$  emission ( $4.04 \text{ kg}_{\text{CO}_2} \text{ kg}_{\text{keratin}}^{-1}$ ), making this process suitable for biomedical and cosmetic applications.

Received 13th March 2023,

Accepted 24th April 2023

DOI: 10.1039/d3gc00850a

[rsc.li/greenchem](https://rsc.li/greenchem)

## Introduction

Ionic liquids (ILs) have garnered intense attention from the academic and industrial research communities due to their high dissolution capability, low volatility, thermal stability, and non-flammability if properly designed. ILs comprise organic cations and organic or inorganic anions, thus displaying low melting temperatures compared to inorganic salts.<sup>1,2</sup>

The history of first generation ILs started in 1914, with the use of “ethyl ammonium nitrates” by Paul Walden.<sup>3</sup> Second-generation ILs, generally represented by imidazolium and alkyl pyridinium, have attracted considerable attention in the last decades. They have been used to dissolve different biopoly-

mers, including cellulose, chitin, silk, lignin, and keratin, which have low solubility in organic solvents.<sup>4–10</sup> Despite the efficient dissolution presented by this class of ILs, some have raised environmental, economic and biocompatibility concerns,<sup>11–14</sup> leading the scientists to investigate the third generation of ILs. Following the 7<sup>th</sup> and 10<sup>th</sup> Green Chemistry principles, this class of ILs is derived from renewable feedstock (e.g. natural sugars and amino acids), and should present low toxicity, high biocompatibility, and biodegradability.<sup>15–18</sup>

Despite their promising properties, bio-based ILs have not been highly investigated, especially for keratin, a protein with interest for use in hydrogels and films for tissue-engineering applications.<sup>19–21</sup> Keratin represents around 90 wt% and 95 wt% of chicken feathers and wool, respectively.<sup>9,21–26</sup> Although wool is the primary source explored for keratin dissolution, the potential production of keratin from chicken feathers is 2.5 times superior to wool.<sup>27</sup> Chicken is one of the most consumed meats in the world, reaching worldwide an annual consumption of 65 million tons, while producing a relevant amount of feathers waste (7 wt% of the total mass of

<sup>a</sup>CICECO – Aveiro Institute of Materials, Department of Chemistry, University of Aveiro, 3810-193 Aveiro, Portugal. E-mail: [maragfreire@ua.pt](mailto:maragfreire@ua.pt)

<sup>b</sup>Department of Chemical Engineering, Imperial College London, South Kensington Campus, London SW7 2AZ, UK. E-mail: [j.hallett@imperial.ac.uk](mailto:j.hallett@imperial.ac.uk)

† Electronic supplementary information (ESI) available. See DOI: <https://doi.org/10.1039/d3gc00850a>



an adult chicken).<sup>27–29</sup> Chicken feathers waste is disposed of through incineration or landfilling, thus largely contributing to environmental pollution.<sup>28,30,31</sup> Therefore, there is a high demand for developing sustainable approaches for feathers waste valorisation.

Keratin has low solubility in traditional organic solvents due to their inter- and intramolecular disulfide bonds.<sup>32,33</sup> As reviewed by Chilakamarry *et al.*,<sup>34</sup> methods such as acid hydrolysis, alkaline hydrolysis, and steam exposure techniques need to be employed. In addition to their hazardous concerns these methods also have negative impacts on keratin structure.<sup>34</sup>

When appropriately designed, ILs allow high keratin dissolution. The study of keratin recovery by ILs started in 2005, dissolving wool in 1-butyl-3-methylimidazolium chloride ([C<sub>2</sub>C<sub>1</sub>im]Cl).<sup>35</sup> More recently, Liu *et al.*<sup>36</sup> used COSMO to evaluate the efficiency of 621 ILs for keratin dissolution. The experimental solubility of wool keratin was evaluated for the most promising ILs; resulting in 35 wt% of wool dissolution by [C<sub>2</sub>C<sub>1</sub>im]Cl at 180 °C, while 38 wt% was dissolved by 1-ethyl-3-methylimidazolium acetate ([C<sub>2</sub>C<sub>1</sub>im][C<sub>1</sub>CO<sub>2</sub>]) at 120 °C. Recently, our group<sup>29</sup> investigated the use of aqueous solutions of imidazolium-based ILs instead of pure ILs for chicken feathers dissolution, further addressing the IL anion effect. An aqueous solution of 1-butyl-3-methylimidazolium acetate (80 wt%), greatly enabled keratin recovery and preparation of keratin biofilms. A keratin film was prepared and its cytotoxicity was investigated in macrophages, monocytes, keratinocytes, and fibroblasts. The keratin film did not present any cytotoxicity for these cells. Satisfactory results of anti-inflammatory activity were obtained as well. Finally, *in vitro* wound healing assays showed that the produced keratin film improves the proliferation of keratinocytes and fibroblasts, accelerating wound healing.<sup>29</sup>

Based on the described promising evidences, we now aim to find a biobased and lower cost IL to produce keratin films viable for biomedical applications. From this perspective, cholinium acetate ([N<sub>111(2OH)</sub>][C<sub>1</sub>CO<sub>2</sub>]) is investigated here, for the first time, for chicken feathers dissolution and keratin recovery. With complete dissolution gained, keratin regeneration conditions were optimized using response surface methodology (RSM) to identify the best protein recovery conditions. Furthermore, the properties of the regenerated keratin were investigated. In addition, and considering the main challenges for ILs in commercial applications (including their relatively high cost and the subsequent requirement of significant ILs recovery and recycling),<sup>1</sup> we evaluated [N<sub>111(2OH)</sub>][C<sub>1</sub>CO<sub>2</sub>] recycling (4 cycles) and performed a techno-economic assessment of the developed keratin recovery process. To the best of our knowledge, no reports have presented the techno-economic impacts of ILs on keratin recovery. Although it is commonly stated that ILs are expensive, there is a lack of understanding from a process-engineering perspective to improve their use in industrial applications, and the use of techno-economic assessments can help identify strong and weak points and motivate both academic research and industrial application of ILs.

## Materials and methods

### Materials

Chicken feathers were collected from the Campoaves company in Oliveira de Frades, Portugal. Chicken feathers were washed three times with soapy water and dried at 50 °C in an air oven (Carbolite Gero) for 72 h. After drying, the chicken feathers were milled and immersed in 99 wt% ethanol for 24 h. The cleaned feathers were dried at 50 °C for 24 h. Finally, the feathers were stored in the refrigerator at 5 °C. [N<sub>111(2OH)</sub>][C<sub>1</sub>CO<sub>2</sub>] (98 wt%) was purchased from IOLITEC. Ethanol (99.8 wt%) was acquired from Fisher Scientific. Chemical reagents used in sodium dodecyl sulfate-polyacrylamide gel electrophoresis (SDS-PAGE) analysis, including urea, hydrochloric acid, tris (hydroxymethyl)-aminomethane (99 wt%) and Page Ruler Low Range Unstained Protein Ladder, were purchased from Thermo Fisher Scientific. Sodium dodecyl sulfate (SDS) and glycerol were from PanReac AppliChem and Biochem Chemopharma, respectively. TEO-Tricine Precast Gels-Run Blue™ (12 wt%, 12-well, 10 × 10 cm) was purchased from Abcam.

### Chicken feathers dissolution

Following the optimization carried out in our previous work,<sup>29</sup> treated chicken feathers were dissolved using an aqueous solution of [N<sub>111(2OH)</sub>][C<sub>1</sub>CO<sub>2</sub>] (80 wt%) in a solid : liquid (chicken feathers : solvent) weight ratio of 1 : 20 w/w, at 100 °C, 650 rpm for 4 h, in a carousel (Carousel Tech, Radleys), with temperature and agitation control.

### Keratin recovery

After chicken feathers dissolution, to achieve keratin precipitation, the coagulant solvent (different concentrations of ethanol) at a desirable solution : coagulant ratio (from 1 : 12.5 to 1 : 1.08 w/w) and time (from 0.64 h to 7.36 h) was added, according to the RSM (detailed information is presented in the following topic). The solution was then centrifugated for 20 min at 25 °C and 4000 rpm in a refrigerator centrifuge machine (Neya 16 R, Remi Elektrotechnik Ltd.), promoting the separation of the precipitated keratin. The protein was collected and washed with water to improve the IL removal, and centrifugated as the previously described conditions. Then, the recovered protein was dried at 50 °C in an air oven for 48 h. The keratin recovery process is schematically summarized in Fig. 1.

The keratin recovery yield (Ker\_RY%) was obtained according to the mass of keratin recovered ( $m_{\text{keratin}}$ ) and mass of chicken feathers used at the dissolution step ( $m_{\text{feathers}}$ ), considering the amount of protein present in the feathers (90 wt%),<sup>29,37</sup> as presented in eqn (1).

$$\text{Ker\_RY}\% = \left( \frac{m_{\text{keratin}}}{(m_{\text{feathers}} \times 0.9)} \right) \times 100 \quad (1)$$

### Response surface methodology

The optimization of the keratin recovery was performed through central composite planning using the RSM 2<sup>3</sup>, with 8



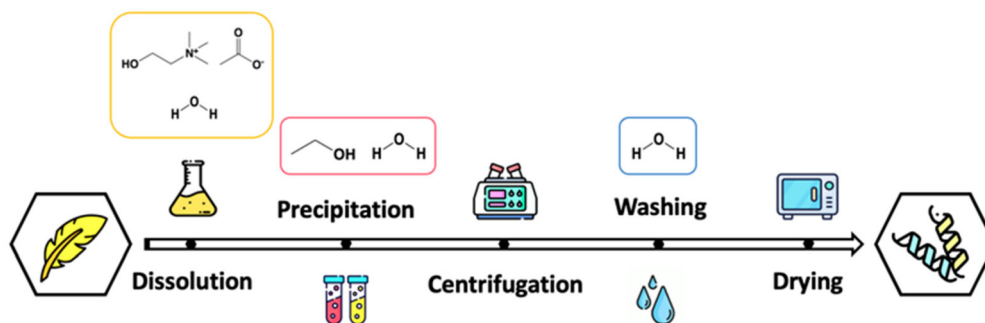


Fig. 1 Schematic representation of the keratin recovery process proposed in this work.

factorial points, 6 axial points, and 3 central point assays. The independent variables (Table 1) were ethanol concentration, time, and solution:coagulant weight ratio, whereas keratin recovery yield (Ker\_RY%) was considered a dependent variable. The surface responses were plotted by changing two variables within the experimental ranges. The results were statistically significant, with a 90% confidence interval ( $p < 0.10$ ).

### Keratin characterization

**SDS-PAGE.** The recovered keratin was dissolved in buffer solution ( $4 \text{ mg mL}^{-1}$ ), formed by  $0.05 \text{ g mol}^{-1}$  Tris-HCl pH 8.0,  $8 \text{ g mol}^{-1}$  urea, and  $0.01 \text{ g mol}^{-1}$  DTT, and stirred for 2 h. The solution was mixed with a running buffer ( $0.5 \text{ g mol}^{-1}$  Tris-HCl pH 6.8, 20 w/w glycerol, 4 w/w SDS, and  $0.01 \text{ g mol}^{-1}$  dithiothreitol (DTT)) and then heated at  $90^\circ\text{C}$  for 5 min to achieve denaturation. The protein marker (3.4 to 100 kDa) and the sample were loaded into the polyacrylamide gels and submitted to a run at 80 V for 1 h, followed by 120 V for 1 h. Then, the proteins were stained with Coomassie Brilliant Blue G-250 overnight at room temperature.<sup>29</sup>

### Fourier transform infrared attenuated total reflectance (FTIR-ATR)

The FTIR-ATR spectra of chicken feathers and recovered keratin obtained with the optimal conditions were acquired in a FTIR system spectrum BX, PerkinElmer, equipped with a single horizontal Golden Gate ATR cell and a diamond crystal. The available functional groups were analyzed at room temperature with controlled air humidity. All data were recorded in a frequency range of  $4000\text{--}400 \text{ cm}^{-1}$  by accumulating 32 scans with a resolution of  $4 \text{ cm}^{-1}$  and an interval of  $1 \text{ cm}^{-1}$ .

Table 1 Levels of process factors in experimental design

| Parameters                     | Levels |       |     |        |        |
|--------------------------------|--------|-------|-----|--------|--------|
|                                | −1.68  | −1    | 0   | 1      | 1.68   |
| Ethanol concentration (%)      | 0      | 20.25 | 50  | 79.75  | 99.98  |
| Time (h)                       | 0.64   | 2.0   | 4.0 | 6.0    | 7.36   |
| Solution:coagulant ratio (w/w) | 1:12.5 | 1:4   | 1:2 | 1:1.33 | 1:1.08 |

### Thermogravimetric analysis (TGA)

Thermogravimetric analyses were carried out in a differential thermogravimetric analyzer Hitachi STA300. The samples were placed in aluminium support and further analyzed under a nitrogen gas blanket using a flow rate of  $1 \text{ mL min}^{-1}$ . The samples were heated at a rate of  $10^\circ\text{C min}^{-1}$  with a temperature range of  $30\text{--}900^\circ\text{C}$ .

### Elemental analysis

The weight percentage (wt%) of carbon (C), hydrogen (H), nitrogen (N) and sulphur (S) of keratin were determined through elemental analysis, using a Truspec 630-200-200 equipment. The combustion furnace temperature was  $1075^\circ\text{C}$  and the subsequent burner temperature was  $850^\circ\text{C}$ . The detection method used for carbon, hydrogen, and sulphur was infrared absorption, while for nitrogen it was used the thermal conductivity method.

### X-ray diffraction (XRD)

XRD analysis was performed using an Empyrean diffractometer with Cu  $K\alpha$  radiation at 45 kV and 40 mA, ranging from  $5^\circ$  to  $90^\circ$  at a rate of  $0.02^\circ$ .

### IL recovery and reuse

To achieve the  $[\text{N}_{111(2\text{OH})}][\text{C}_1\text{CO}_2]$  recovery and reuse, after the centrifugation and washing steps, the supernatants were collected and transferred to a clean round bottomed flask, previously weighed. The volatile compounds were removed from the solution using a rotatory evaporator R-10, heating bath B-491, vacuum pump V-700 and vacuum controller V-850 (all from Buchi, Switzerland). The purity of the IL was determined by measuring the water content in the obtained IL, using a V20 Volumetric Karl-Fischer titrator (Mettler Toledo). The mass of IL recovered ( $m_R$ ), the mass of IL used at the dissolution step ( $m_0$ ) and the purity of IL ( $\%_{\text{IL}}$ ) were used to determine the IL recovery yield (IL\_RY), as presented in eqn (2). The IL recycling and reuse were evaluated for a total of 4 dissolution and recovery cycles.

$$\text{IL\_RY}(\%) = \left( \frac{(m_R \times \%_{\text{IL}})}{m_0} \right) \times 100 \quad (2)$$

### Process simulation at Aspen Plus

In order to study the most significant limitations of cost-effective keratin recovery using the aqueous solution of



$[N_{111(2OH)}][C_1CO_2]$ , a process simulation was carried out at Aspen Plus V11 for process modelling with the integrated Aspen Economics package for the estimation of the purchased and installed costs of the plant with same principles reported in previous publications.<sup>38–40</sup> The reactors used for the chicken feathers dissolution and keratin recovery have been approximated as flash vessels. Due to the batch operation, three reactor units were considered to compensate for the filling, reaction, and discharging time, guaranteeing a continuous process. Methodologies for implementing the IL follow the procedure previously reported.<sup>38,39</sup>

Quantum chemical calculations to create the chemical structure of the compounds were done using TURBOMOLE v7.02 (with TmoleX v4.5.2 graphic interface) software. The molecular structures of the compounds were optimized until their minimum energy level. The quantum chemical calculations were carried out to generate a COSMO file. The standard method in COSMOtherm is B88-P86 (bp) functional and TZVP basis with RI approximation using the COSMO solvation model. Through these quantum chemical calculations, a COSMO file was created containing energies, geometries, and polarization charge of the  $\sigma$ -surface.

COSMO-RS method program package (version C30\_1904) and its parametrization BP\_TZVP\_C30\_19 were used in COSMOtherm software. COSMO-RS method was used to create pseudo components into Aspen Properties, and COSMOtherm was used to complete the usual boiling point (NBP), density,  $\sigma$ -profile, and COSMO-volume calculations (the last two to use the COSMOSAC model from Aspen Properties).

To implement the IL into the ASPEN PLUS v11 simulator, a property package was created in Aspen Properties v11. Compounds were defined as pseudo components. Usual boiling point, density, and molecular weight were the information imported from COSMOtherm to make the pseudo component. The COSMOSAC model was selected as a thermodynamic model, and the gamma method was modified to use COSMOSAC-Mathias modification.  $\sigma$ -Profile was specified as pure component properties SGPRF1-5 and COSMO-volume as CSACVL component parameter.

### Economic and environmental evaluation

Since the process requires refrigeration for the keratin recovery, cost and CO<sub>2</sub> emissions associated with the use of a refrigerant were estimated based on a previous publication based on an ammonia compression cycle.<sup>41</sup> In this process, ammonia vapor is compressed through a compressor fed with electricity to increase the boiling point so that ammonia can be condensed with cooling water. The liquid ammonia is expanded with a valve to decrease the boiling point to a level required for the unit operation. The parameters were chosen as reference for an ammonia compression cycle working at 12 bar and 40 °C in the condenser and supplying refrigeration at 5 °C in the evaporator. The parameters used to estimate the contribution of a refrigeration system, as well the other costs (utility, capital, operating and fixed costs) involved in this process, are presented in the ESI (Tables S1–S4<sup>†</sup>), according to

the typical engineering parameters reported in the literature.<sup>42</sup> Labour cost (LC) was estimated considering 30 operators with 50 000 \$ per year of salary. CO<sub>2</sub> emissions were estimated considering that steam and electricity are produced through burning methane considering 80% thermal efficiency for steam generation and 45% for electricity.<sup>41</sup> The minimum selling price was calculated considering the total operating costs, annual plant depreciation, and keratin productivity.

## Results and discussion

### Optimization of operational conditions by RSM

We aimed to develop a sustainable process for keratin recovery from chicken feathers waste, in which an aqueous solution of  $[N_{111(2OH)}][C_1CO_2]$  (80 wt%) was used. After achieving complete chicken feathers dissolution (in a solid : liquid weight ratio of 1 : 20 w/w, at 100 °C, 650 rpm for 4 h), several recovery conditions were investigated to improve the recovered keratin yield, namely ethanol concentration in water ( $X_1$ ), time ( $X_2$ ), and solution : coagulant ratio ( $X_3$ ). The obtained results are presented in Table S5.<sup>†</sup>

The RSM allows the identification of possible mutual effects and interactions between the three variables investigated on keratin recovery. Fig. 2A illustrates the plots of the response surface results, while Fig. 2B shows the contour graph with simultaneous interaction between every two independent variables in the keratin recovery yield.

The response surfaces show an increase in keratin yield when the ethanol concentration is low (around 20.25 wt%), revealing that the capacity to recover keratin will increase by increasing the water concentration. This indicates that water is better at creating H-bonds with  $[N_{111(2OH)}][C_1CO_2]$ , enabling protein precipitation. The strong influence of coagulant is an expected trend, as previously observed by other authors.<sup>29,43</sup> Concerning the time, at least 4 h are necessary to achieve a higher keratin yield. Increasing the solution : coagulant ratio from 0.13 to 0.88 ( $\pm 1 : 12.5$  to  $1 : 1.08$ ) also improves keratin yield, indicating that it is required to use a ratio lower than 1 : 2 w/w.

Analysis of variance (ANOVA) was used to determine the statistical significance of the variables and their interactions. The efficiency of keratin recovery was used as a dependent variable in the definition of the predictive model represented by eqn (S1) in the ESI.<sup>†</sup> The model was adjusted with a confidence level of 90% and can be considered a good predictive model. The statistical analysis and data shown in Fig. S1 in the ESI<sup>†</sup> indicate that the linear and quadratic effects of all variables are significant in this process, as well as the interaction between ethanol concentration and solution : coagulant ratio. The model was validated using the plot of the observed values *versus* predicted values, demonstrating a satisfactory description of the experimental results.

According to the RSM optimization, the optimal conditions for keratin recovery are 20.25 wt% of ethanol in water, 5 h, and solution : coagulant ratio of 1 : 1.45 w/w. At the optimized con-





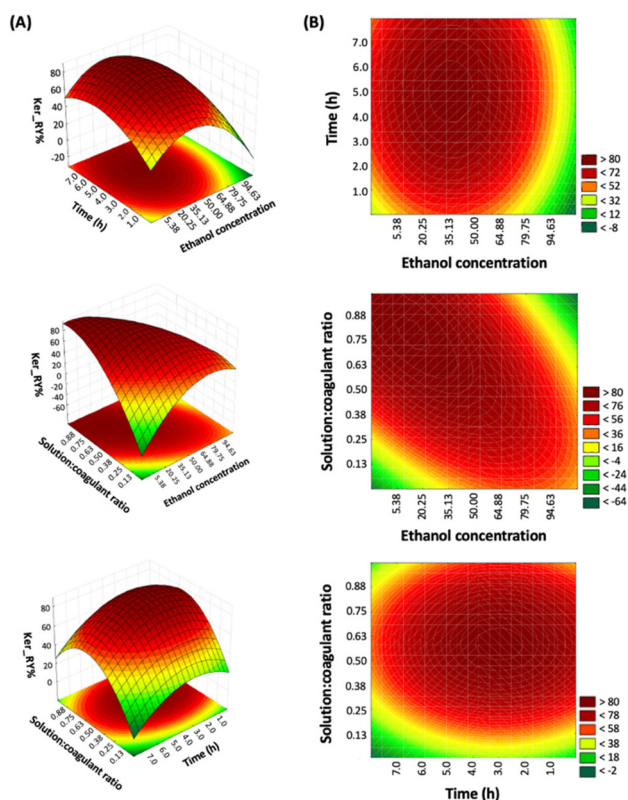


**Fig. 2** Surface graphs (A) and contour graphs (B) of the interactions of different variables in the keratin recovery: (i) time and ethanol concentration, (ii) solution : coagulant ratio and ethanol concentration, and (iii) solution : coagulant ratio and time.

ditions of the experimental design, a keratin yield of  $(93 \pm 4)$  wt% was obtained. This value is in line with the predicted result (97%) obtained using eqn (S1) given in the ESI†. The keratin recovery yield obtained here is higher compared with published results using other ILs, including the 90 wt% of keratin yield obtained from an aqueous solution of  $[C_4C_1im][C_1CO_2]$ ,<sup>29</sup> and 72 wt% from an aqueous solution of tetramethyl ammonium hydroxide.<sup>44</sup> In addition, it is essential to highlight that we used a bio-based IL, presenting high biodegradability and low toxicity,<sup>16,45,46</sup> which can overcome some of the concerns related to the second generation of ILs.<sup>14,45,47</sup>

### Characterization of the recovered keratin

The keratin sample obtained using the optimal recovery conditions (20.25 wt% of ethanol in water, 5 h, and solution : coagulant ratio of 1 : 1.45 w/w) and chicken feathers were analysed by FTIR, SDS-PAGE, and TGA to determine their properties and thus appraise the potential application of the recovered keratin.

The functional groups of chicken feathers and recovered keratin are presented in Fig. 3. The absorption peaks obtained for chicken feathers and keratin corresponds to  $3278\text{ cm}^{-1}$  and  $3274\text{ cm}^{-1}$  (amide A),  $1632\text{ cm}^{-1}$  and  $1640\text{ cm}^{-1}$  (amide I),

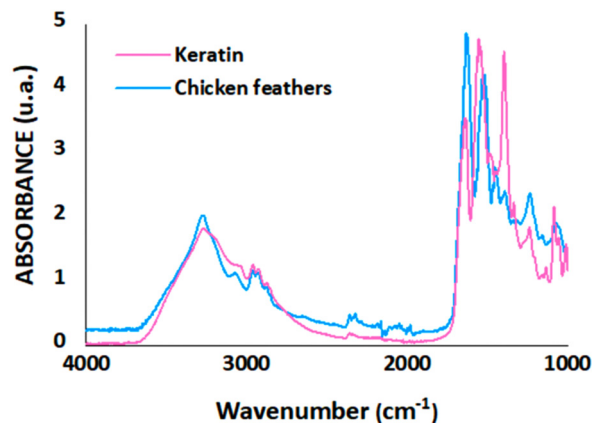


**Fig. 3** FTIR spectra of chicken feathers and keratin recovered using the optimal condition (20.25 wt% of ethanol concentration, 5 h, and solution : coagulant ratio of 1 : 1.45).

$1518\text{ cm}^{-1}$  and  $1552\text{ cm}^{-1}$  (amide II), and  $1239\text{ cm}^{-1}$  and  $1232\text{ cm}^{-1}$  (amide III), respectively. The peaks observed here follow the results reported in the literature for amide A, amide I, amide II and amide III, corresponding to peaks between  $3650$  and  $2750\text{ cm}^{-1}$ ,  $1750$ – $1570\text{ cm}^{-1}$ ,  $1570$ – $1470\text{ cm}^{-1}$ , and  $1300$ – $1180\text{ cm}^{-1}$ , respectively.<sup>10,48</sup> In general, both samples presented the same peaks, except for the high intensity of the peak observed for keratin samples between  $1430$ – $1320\text{ cm}^{-1}$  (O–H bending), representing the presence of the IL in the recovered keratin. It is essential to highlight that, despite this IL does not indicate possible contamination for biomaterials application due to its biocompatible features,<sup>16</sup> it is indispensable to investigate its effects for the desired application.

The molecular weight of the keratin sample obtained with the optimal conditions was obtained by SDS-PAGE (Fig. S3 in the ESI†). In summary, a band around 5 to 12 kDa is observed, in accordance with the literature and the molecular weight expected for keratin from chicken feathers ( $\sim 10\text{ kDa}$ ).<sup>24,31</sup>

Thermal stability of keratin and chicken feathers was assessed by TGA. As shown in Fig. 4, the profiles present a similar pattern with two-step degradations. The first peak corresponds to water loss (representing around 10% of weight). The second peak corresponds to keratin degradation, which is associated with the denaturation of the secondary structure of the protein. The thermal stability of keratin ( $\sim 190^\circ\text{C}$ ) is lower than that of chicken feathers ( $\sim 220^\circ\text{C}$ ), which can be due to the effect of the dissolution step with the  $[N_{111}(20H)][C_1CO_2]$ , since this decrease was not observed for keratin dissolved with  $[C_4C_1im][C_1CO_2]$ .<sup>29</sup> The thermal stability is consistent with results reported in the literature ( $200$ – $230^\circ\text{C}$ ).<sup>24,48</sup> In general, the still high degradation temperature of keratin ( $\sim 190^\circ\text{C}$ ) obtained in this work is highly relevant from an application point of view, supporting its use in the envisioned biomedical applications.

Elemental analysis was carried out to determine the content of carbon, hydrogen, nitrogen and sulphur in the recovered keratin. This sample comprises 49.39 wt% of C,



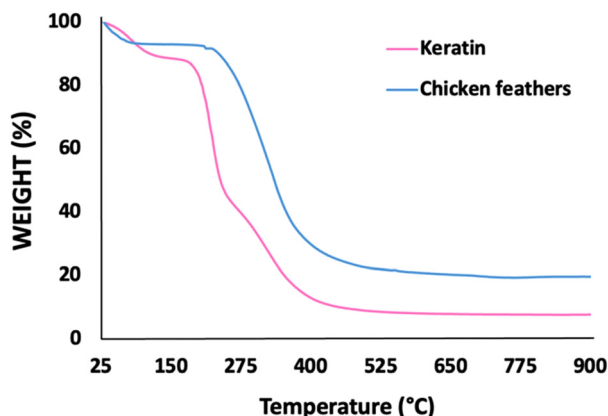


Fig. 4 Thermal stability of keratin and chicken feathers.

7.29 wt% of H, 14.90 wt% of N, and 1.23 wt% of S. The presence of N in the keratin sample is due to the peptide bonds, while the presence of S is linked to the cysteine amino acid responsible for the sulphur–sulphur bonding on the keratin structure.<sup>49</sup> These results are comparable to those reported in the literature for other keratin samples from chicken feathers.<sup>43,49</sup>

Fig. 5 shows the XRD spectrum of the recovered keratin, with diffraction peaks appearing between 5° and 14° and 15° and 25°. The diffraction peak at 10° corresponds to the protein  $\alpha$ -helix structure, while the diffraction peak at 20° is related to the  $\beta$ -sheet structure of keratin, being in accordance with the literature.<sup>50,51</sup>

### Ionic liquid recovery

Regardless of the feasibility of the keratin recovery process using an aqueous solution of IL,  $[N_{111}(2OH)][C_1CO_2]$  recovery and reuse is as a prerequisite condition for developing a sustainable process. Accordingly, this work attempted the IL reuse in 4 cycles of dissolution with fresh biomass. The process was performed at the optimized conditions (20.25 wt% of ethanol concentration, 5 h, and solution:coagulant ratio of 1:1.45 w/w) to accomplish this goal. All feathers components were

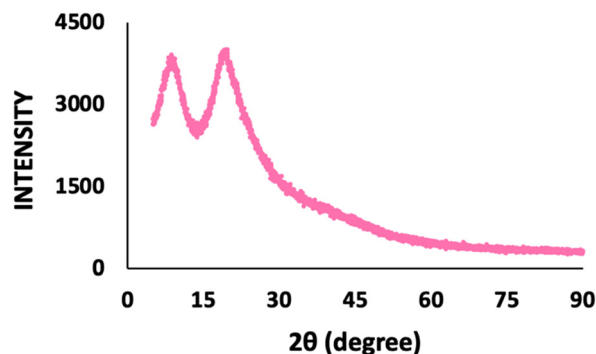


Fig. 5 XRD spectrum of the recovered keratin under the optimal conditions.

dissolved into the aqueous solution of  $[N_{111}(2OH)][C_1CO_2]$  and eliminated by the coagulant solvent addition, without presenting any effects in the keratin recovery performance, suggesting that the protein that was not recovered could still remain in the coagulant solution.

Fig. 6 depicts the IL recovery efficiency. As expected, the higher amount of IL (~88 wt%) comes from the precipitation step. In addition, a significant amount of IL is recycled from the first washing (~5 wt%) and a small amount from the subsequent washings (~1 wt%). The necessity of several washing steps is probably due to the high viscosity of  $[N_{111}(2OH)][C_1CO_2]$ , which maintains a strong hydrogen bonding network with keratin.<sup>52</sup> Approximately  $(93 \pm 4)$  wt% to  $(86 \pm 2)$  wt% of keratin was recovered along the 4 cycles, indicating that the reused IL does not have a significant impact at keratin recovery efficiency. The integrity of the recycled IL was confirmed by  $^1H$  and  $^{13}C$  NMR, as shown in the ESI (Fig. S4–S7†), revealing that no solvent degradation occurs under the conditions used in this work.

### Techno-economic assessment

In order to establish a green process, the economic and environmental impact of  $[N_{111}(2OH)][C_1CO_2]$  recycling was evaluated. The IL recovery obtained in this work equals  $(95 \pm 1)\%$  for 4 cycles. Nevertheless, having in mind that IL losses on a laboratory scale are higher (due to the sample transfer between flasks) than on an industrial scale, and considering the higher efficiency of IL recovery in a continuous process, here we considered a total IL recovery for the techno-economic assessment.

Since keratin recovery requires adding an aqueous solution of ethanol, the process will need the energy to restore the IL at the right composition to be suitable for a further cycle. The experimental values reported in previous sections were used to evaluate the heat duty to boil ethanol and water mixture from the liquor. The process flow diagram is presented in Fig. 7. The IL feed ( $1000 \text{ kg h}^{-1}$ ) with chicken feathers at a loading of 5% is heated to 100 °C for 4 h (EXT-KER). Then, a stream of

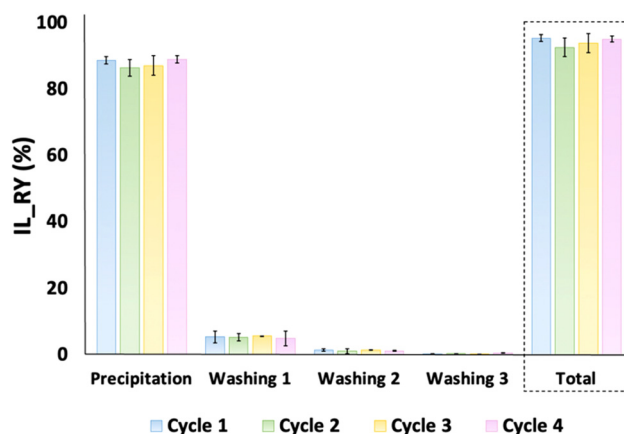


Fig. 6 Evaluation of  $[N_{111}(2OH)][C_1CO_2]$  recovery and recycling for 4 cycles.



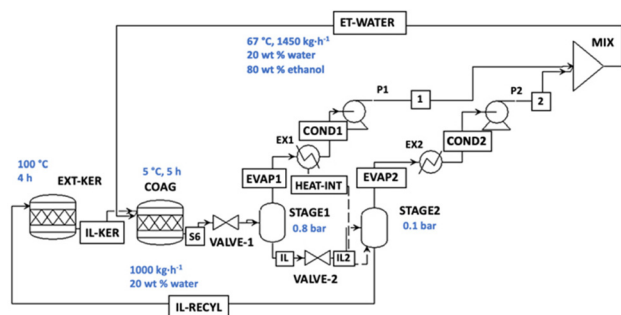


Fig. 7 Process flow diagram used for the simulation of the keratin recovery using the  $[N_{111}(2OH)][C_1CO_2]$  aqueous solution.

1450 kg h<sup>-1</sup> with 20.25 wt% of ethanol is introduced as a coagulant solvent, cooled with a refrigerant, and let settle for 5 h (COAG).

Multiple-effect evaporators were used for IL regeneration. According to previous reports,<sup>38,39,41</sup> three-stage evaporators proved to be the best compromise for the regeneration of the IL in different biomass-based processes. Through trial and error, we optimized the process with two-step evaporation at 0.8 and 0.1 bar exploiting the lower boiling point due to the azeotrope formed between water and ethanol and guaranteeing a minimum temperature difference of 5 °C for heat integration. The vapours generated are condensed and recycled in the coagulant reactor (COAG), while the IL with 20 wt% water content is recycled in the main reactor (EXT-KER). The results of the contributions of the different factors affecting the minimum selling price are reported in Fig. 8.

According to our process simulation, the process has a positive CO<sub>2</sub> emission of about 4.04 kg<sub>CO<sub>2</sub></sub> kg<sub>keratin</sub><sup>-1</sup>, mainly due to the unavailability of heat sources in the process in contrast to typical biomass-based approaches. However, considering the renewable raw material used, the product will not produce excess CO<sub>2</sub> at its end of life. The minimum selling price obtained is 22 \$ per kg, calculated considering the total productivity of 350 tons of keratin per year based on the IL flow rate. The price makes this process suitable for keratin use in speciality applications such as personal care and biomedical, but not suitable as a replacement for polyesters and commodity products.

Regarding the price of  $[N_{111}(2OH)][C_1CO_2]$ , it is not considered a limiting factor since it can be easily synthesized using acetic acid and cholinium hydroxide in an acid-base reaction, which makes this IL more accessible.<sup>52</sup> Nevertheless, the operating costs associated with its recovery significantly impact the process. The main contribution to the cost is the steam used to regenerate the IL in the multiple effect evaporator and the capital required for a plant with large flow rates with relatively low productivity (Table S8 in the ESI†). Therefore, new methods for IL recovery deserve to be investigated to increase even more the sustainable character of the developed process.

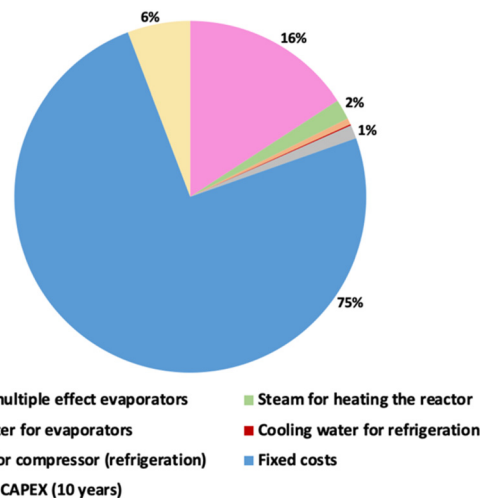


Fig. 8 Contributions to the minimum selling price of keratin.

## Conclusions

Chicken feathers are a large-scale waste generated worldwide which can be used as a source of keratin, with the potential for biomedical applications. In this work, an aqueous solution of  $[N_{111}(2OH)][C_1CO_2]$  was used to achieve the complete dissolution of chicken feathers. By a RSM, the optimal recovery conditions identified to improve the keratin recovery efficiency were 20.25 wt% of ethanol, 5 h, and solution : coagulant ratio of 1 : 1.45 w/w, leading to a keratin recovery yield of (93 ± 4) wt%.  $[N_{111}(2OH)][C_1CO_2]$  was recovered and reused at least four times, achieving around 95 wt% of IL recovery yield at the lab scale and with no significant losses in the keratin recovery yield. Overall, considering the simple synthesis of  $[N_{111}(2OH)][C_1CO_2]$  and its green properties – biocompatibility and low toxicity – principally when compared to imidazolium-based ILs, the proposed process is more sustainable than others previously reported.

Techno-economic analysis indicates that the IL recovery can indeed make the keratin recovery process using  $[N_{111}(2OH)][C_1CO_2]$  cost-competitive for biomedical and cosmetic applications, establishing a path to commercialization for this biomaterial with a minimum selling price of 22 \$ per kg. Concerning the CO<sub>2</sub> emissions, around 4.04 kg<sub>CO<sub>2</sub></sub> kg<sub>keratin</sub><sup>-1</sup> is generated, which is a positive value in contrast to typical biomass-based approaches.

Considering that the IL recovery has a significant impact on the process cost, less expensive methods for the IL recovery deserve to be investigated in the future. Furthermore, taking into account the successful use of  $[N_{111}(2OH)][C_1CO_2]$  aqueous solutions in the keratin recovery from chicken feathers, further research should consider the same solvents to recover keratin from other types of waste, *e.g.* hooves, horns and hair. Among feather waste, other types can be investigated as well, namely duck and turkey feathers. Finally, it is crucial to investigate target biological activities and cytotoxicity towards some cell



lines of the recovered keratin to support its potential in biomedical and cosmetic applications.

## Author contributions

Conceptualization, C. P., J. H., A. G., H. P., J. A. P. C. and M. G. F.; methodology C. P. and A. G.; writing – original draft preparation, C. P.; writing – review and editing, J. H., H. P., J. A. P. C. and M. G. F.; supervision, J. H., H. P., and M. G. F.; funding acquisition, M. G. F.; project administration, M. G. F. All authors listed have made a substantial, direct, and intellectual contribution to the work and agreed to the published version of the manuscript.

## Conflicts of interest

There are no conflicts to declare.

## Acknowledgements

This work was developed within the scope of the project CICECO-Aveiro Institute of Materials, UIDB/50011/2020, UIDP/50011/2020 & LA/P/0006/2020, financed by national funds through the FCT/MCTES (PIDDAC). C. Polesca acknowledges FCT – Fundação para a Ciência e a Tecnologia for the Ph.D. grant with the reference UI/BD/151282/2021. H. Passos acknowledges FCT, I.P., for the researcher contract CEECIND/00831/2017, under the Scientific Employment Stimulus-Individual Call, 2017.

## References

- C. Polesca, H. Passos, J. A. P. Coutinho and M. G. Freire, *Curr. Opin. Green Sustainable Chem.*, 2022, **37**, 100675.
- X. Liu, Y. Nie, X. Meng, Z. Zhang, X. Zhang and S. Zhang, *RSC Adv.*, 2017, **7**, 1981–1988.
- N. Nasirpour, M. Mohammadpourfard and S. Z. Heris, *Chem. Eng. Res. Des.*, 2020, **160**, 264–300.
- N. A. Samsudin, F. W. Low, Y. Yusoff, M. Shakeri, X. Y. Tan, C. W. Lai, N. Asim, C. S. Oon, K. S. Newaz, S. K. Tiong and N. Amin, *J. Mol. Liq.*, 2020, **308**, 113030–113037.
- J. Stanton, Y. Xue, P. Pandher, L. Malek, T. Brown, X. Hu and D. Salas-de la Cruz, *Int. J. Biol. Macromol.*, 2018, **108**, 333–341.
- J. L. Shamshina, O. Zavgorodnya, H. Choudhary, B. Frye, N. Newbury and R. D. Rogers, *ACS Sustainable Chem. Eng.*, 2018, **6**, 14713–14722.
- W. C. Tu and J. P. Hallett, *Curr. Opin. Green Sustainable Chem.*, 2019, **20**, 11–17.
- A. Brandt, J. Gräsvik, J. P. Hallett and T. Welton, *Green Chem.*, 2013, **15**, 550–583.
- R. Li and D. Wang, *J. Appl. Polym. Sci.*, 2013, **127**, 2648–2653.
- A. Idris, R. Vijayaraghavan, U. A. Rana, D. Fredericks, A. F. Patti and D. R. MacFarlane, *Green Chem.*, 2013, **15**, 525–534.
- A. Tarannum, J. R. Rao and N. N. Fathima, *Int. J. Biol. Macromol.*, 2022, **209**, 498–505.
- J. Flieger and M. Flieger, *Int. J. Mol. Sci.*, 2020, **21**, 1–41.
- A. R. P. Gonçalves, X. Paredes, A. F. Cristino, F. J. V. Santos and C. S. G. P. Queirós, *Int. J. Mol. Sci.*, 2021, **22**, 5612.
- S. Ostadjoo, P. Berton, J. L. Shamshina and R. D. Rogers, *Toxicol. Sci.*, 2018, **161**, 249–265.
- D. Mondal, M. Sharma, M. V. Quental, A. P. M. Tavares, K. Prasad and M. G. Freire, *Green Chem.*, 2016, **18**, 6071–6081.
- J. M. Gomes, S. S. Silva and R. L. Reis, *ACS Sustainable Chem. Eng.*, 2020, **8**, 13507–13516.
- C. P. Song, R. N. Ramanan, R. Vijayaraghavan, D. R. Macfarlane, E. S. Chan and C. W. Ooi, *ACS Sustainable Chem. Eng.*, 2015, **3**, 3291–3298.
- A. R. F. Carreira, T. Veloso, N. Schaeffer, J. L. Pereira, S. P. M. Ventura, C. Rizzi, J. S. Plénet, H. Passos and J. A. P. Coutinho, *Molecules*, 2021, **26**, 6958–6976.
- R.-R. Yan, J.-S. Gong, C. Su, Y.-L. Liu, J.-Y. Qian, Z.-H. Xu and J.-S. Shi, *Appl. Microbiol. Biotechnol.*, 2022, **106**, 2349–2366.
- M. Borrelli, N. Joepen, S. Reichl, D. Finis, M. Schoppe, G. Geerling and S. Schrader, *Biomaterials*, 2015, **42**, 112–120.
- N. Ramakrishnan, S. Sharma, A. Gupta and B. Y. Alashwal, *Int. J. Biol. Macromol.*, 2018, **111**, 352–358.
- I. Sinkiewicz, A. Śliwińska, H. Staroszczyk and I. Kołodziejaska, *Waste Biomass Valorization*, 2017, **8**, 1043–1048.
- Y. X. Wang and X. J. Cao, *Process Biochem.*, 2012, **47**, 896–899.
- F. Pourjavaheri, S. O. Pour, O. A. H. Jones, P. M. Smooker, R. Brkljača, F. Sherkat, E. W. Blanch, A. Gupta and R. A. Shanks, *Process Biochem.*, 2019, **82**, 205–214.
- A. Idris, R. Vijayaraghavan, U. A. Rana, A. F. Patti and D. R. MacFarlane, *Green Chem.*, 2014, **16**, 2857–2864.
- S. Zheng, Y. Nie, S. Zhang, X. Zhang and L. Wang, *ACS Sustainable Chem. Eng.*, 2015, **3**, 2925–2932.
- B. Mu, F. Hassan and Y. Yang, *Green Chem.*, 2020, **22**, 1726–1734.
- T. Tesfaye, B. Sithole and D. Ramjugernath, *Sustainable Chem. Pharm.*, 2018, **8**, 38–49.
- C. Polesca, H. Passos, B. M. Neves, J. A. P. Coutinho and M. G. Freire, *Green Chem.*, 2023, **25**, 1424–1434.
- S. I. N. Ayutthaya, S. Tanpichai and J. Wootthikanokkhan, *J. Polym. Environ.*, 2015, **23**, 506–516.
- N. B. Kamarudin, S. Sharma, A. Gupta, C. G. Kee, S. M. S. B. T. Chik and R. Gupta, *3 Biotech.*, 2017, **7**, 1–9.
- E. M. Nuutinen, P. Willberg-Keyriläinen, T. Virtanen, A. Mija, L. Kuutti, R. Lantto and A. S. Jääskeläinen, *RSC Adv.*, 2019, **9**, 19720–19728.
- R. K. Donato and A. Mija, *Polymers*, 2020, **12**, 1–64.





- 34 C. R. Chilakamarthy, S. Mahmood, S. N. B. M. Saffe, M. A. B. Arifin, A. Gupta, M. Y. Sikkandar, S. S. Begum and B. Narasaiah, *3 Biotech.*, 2021, **11**, 1–12.
- 35 H. Xie, S. Li and S. Zhang, *Green Chem.*, 2005, **7**, 606–608.
- 36 X. Liu, Y. Nie, Y. Liu, S. Zhang and A. L. Skov, *ACS Sustainable Chem. Eng.*, 2018, **6**, 17314–17322.
- 37 T. Tesfaye, B. Sithole, D. Ramjugernath and V. Chuniwall, *Waste Manage.*, 2017, **68**, 626–635.
- 38 A. R. Abouelela, A. Al-Ghatta, P. Verdía, M. S. Koo, J. Lemus and J. P. Hallett, *ACS Sustainable Chem. Eng.*, 2021, **9**, 10524–10536.
- 39 A. Al-Ghatta, J. D. E. T. Wilton-Ely and J. P. Hallett, *ACS Sustainable Chem. Eng.*, 2019, **7**, 16483–16492.
- 40 C. M. P. Freitas, D. B. S. Júnior, R. D. Martins, M. M. S. Dias, J. S. R. Coimbra and R. C. S. Sousa, *Bioprocess Biosyst. Eng.*, 2021, **44**, 1639–1647.
- 41 A. Al-Ghatta, J. D. E. T. Wilton-Ely and J. P. Hallett, *Green Chem.*, 2021, **23**, 1716–1733.
- 42 M. R. Shabani and R. B. Yekta, *Cost Eng.*, 2006, **48**, 22–25.
- 43 O. D. Fagbemi, B. Sithole and T. Tesfaye, *Sustainable Chem. Pharm.*, 2020, **7**, 100267.
- 44 T. K. Maity, N. Singh, P. Vaghela, A. Ghosh, S. Singh, P. B. Shinde, R. A. Sequeira and K. Prasad, *Sustainable Environ. Res.*, 2022, **32**, 42.
- 45 I. F. Mena, E. Diaz, J. Palomar, J. J. Rodriguez and A. F. Mohedano, *Chemosphere*, 2020, **240**, 124947.
- 46 F. Elhi, H. Priks, P. Rinne, N. Kaldalu, E. Žusinaite, U. Johanson, A. Aabloo, T. Tamm and K. Põhako-Esko, *Smart Mater. Struct.*, 2020, **29**, 055021.
- 47 J. Flieger and M. Flieger, *Int. J. Mol. Sci.*, 2020, **21**, 6267–6308.
- 48 B. Ma, X. Qiao, X. Hou and Y. Yang, *Int. J. Biol. Macromol.*, 2016, **89**, 614–621.
- 49 Y. Estévez-Martínez, C. Velasco-Santos, A. L. Martínez-Hernández, G. Delgado, E. Cuevas-Yáñez, D. Alaníz-Lumbreras, S. Duron-Torres and V. M. Castaño, *J. Nanomater.*, 2013, 702157.
- 50 W. Du, L. Zhang, C. Zhang, J. Cao, D. Wang, H. Li, W. Li and J. Zeng, *Front. Mater.*, 2021, **8**, 789081.
- 51 A. Valkov, M. Zinigrad, A. Sobolev and M. Nisnevitch, *Int. J. Mol. Sci.*, 2020, **21**, 3512.
- 52 A. Ovejero-Pérez, M. Ayuso, V. Rigual, J. C. Domínguez, J. García, M. V. Alonso, M. Oliet and F. Rodriguez, *ACS Sustainable Chem. Eng.*, 2021, **9**, 8457–8476.

